Journal of Materials Science and Chemical Engineering, 2018, 6, 55-67
http://www.scirp.org/journal/msce
ISSN Online: 2327-6053
ISSN Print: 2327-6045

Effect of Pre-Ageing on the Precipitation Behaviors and Mechanical Properties of Al-7Si-Mg Alloys

Wen-Chi Chen[1], Sheng-Lon Lee[1], An-Hung Tan[2*]

[1]Department of Mechanical Engineering, National Central University, Taiwan
[2]Department of Mechanical Engineering, Chien Hsin University, Taiwan
Email: *ahtan@uch.edu.tw

How to cite this paper: Chen, W.-C., Lee, S.-L. and Tan, A.-H. (2018) Effect of Pre-Ageing on the Precipitation Behaviors and Mechanical Properties of Al-7Si-Mg Alloys. *Journal of Materials Science and Chemical Engineering*, **6**, 55-67.
https://doi.org/10.4236/msce.2018.63005

Received: February 14, 2018
Accepted: March 23, 2018
Published: March 26, 2018

Abstract

For alloys that are quenched to 25˚C room temperature, there are Mg-Mg, Si-Si and Mg-Si clusters shown by exothermic peaks in a A357 alloy. However, there are no clear Mg-Mg, Si-Si and Mg-Si cluster exothermic peaks in a A356 alloy. Hence, the low Mg content in a A356 alloy has less impact with natural ageing. The natural ageing impact on the mechanical properties of a A357 alloy is higher than a A356 alloy due to the precipitation of Mg-Si clusters for which the nucleation size does not reach the critical size. The 90˚C pre-ageing process could promote Mg-Si clusters to a critical size to become the nucleation site for of β'. This then increases the artificial ageing strength and mitigates the impact of natural ageing.

Keywords

Pre-Ageing, Precipitation, Mechanical Property, Al-7Si-Mg Alloys

1. Introduction

A356 and A357 aluminum casting alloys are widely used in the automotive and aerospace industries due to their good castability, wearability, corrosion resistance, weldability, and good strength to weight ratio etc. A356 and A357 alloys are heat treatable Al-Si-Mg hypoeutectic alloys. T6 artificial ageing can enhance their strength and hardness. This major heat treatment procedure includes solution treatment, quenching and artificial ageing. However, there is usually a waiting time between quenching and artificial ageing due to production schedule arrangements that will impact the follow up artificial mechanical strength. This waiting time was called pre-ageing. Natural ageing is pre-ageing at room temperature.

Banhart [1] has summarized the Al-Mg-Si alloy precipitation sequence as shown in **Figure 1**. The Mg and Si atoms, which are decomposed to be independent atoms, are dispersed in an aluminum matrix when in a supersaturated solid solution (SSSS) process. When pre-ageing, Mg and Si atoms are attracted by each other to become Mg-Mg and Si-Si clusters first. Then, Mg and Si co-cluster to form GP(I) precipitation. Sometimes, it is called initial-β'. GP(I) zones either further evolve directly to a phase β' and then to a number of other meta stable phases labeled β, B', U1, U2 (another one, U3, has been postulated theoretically). The final equilibrium phase β is reached for higher ageing temperatures only.

The natural ageing or higher temperature pre-ageing which initiates the cluster precipitation process is studied by a 3 dimensional atomic probe (3DAP)/atom-probe field ion microscope (APFIM) and a transmission electron microscope (TEM) [2] [3] [4]. The Mg-Mg, Si-Si and Si-Mg cluster ratio are investigated with quench, 1 week natural ageing and 8 hour 90˚C pre-ageing on an Al-Mg-Si 6061 alloy. Mg-Mg and Si-Si spherical shape clusters are formed during or immediately after quenching. The Mg-Mg cluster ratio is higher than the Si-Si and Mg-Si ratios after quenching. After 1 week natural ageing, the Mg-Mg and Si-Mg cluster ratio are reduced. The Si-Si cluster ratio is higher than Mg-Mg and Si-Mg clusters. When quenched to 90˚C with 1 week 25˚C pre-ageing, the Si-Si cluster ratio is similar to a quench of 25˚C with 1 week 25˚C natural ageing, but the Mg-Mg and Mg-Si clusters ratio is higher than with quenching [2]. The Mg-Mg clusters tend to dissolve at 70˚C - 90˚C which leads to Si-Mg needle shape cluster formation where they may act as preferential heterogeneous nucleation sites to a higher density of β'' hardening particles [2] [3]. Natural ageing will suppress Mg-Si cluster precipitation kinetics to reduce β' precipitates [2]. Sha [4] reported a similar result on a F357 Al-7Si-0.6Mg alloy. Natural ageing will not change the precipitation sequence of the alloy. However, natural pre-ageing slows down the precipitation during an initial 1 hr of artificial ageing. The number density of β'-needles formed in the primary α-Al grains of the 120

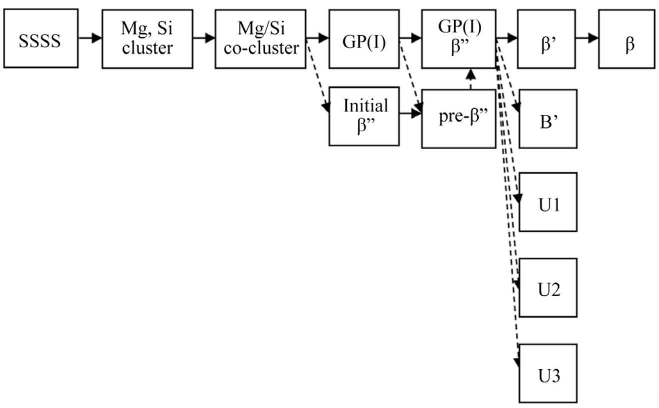

Figure 1. Sequence of phases found during age hardening of Al-Mg-Si alloys.

hours naturally pre-aged sample is approximately half of what is seen with a quenched sample.

Differential scanning calorimetry (DSC), APFIM/3DAP and TEM were used to study Al-Mg-Si and Al-Si-Mg alloy pre-ageing and artificial ageing. Mg is incorporated into the Si clusters very early in the precipitation sequence. The initial stage of precipitation during ageing of alloy 6061 at 70˚C involves the formation of small, separate Si and Mg rich clusters, then followed by movement of Mg atoms to the Si clusters [5]. The Al-Mg-Si alloy precipitation sequence is as follows: independent clusters of Mg and Si atoms→co-clusters that contain Mg and Si atoms→small precipitates of unknown structure→β' needle-shape precipitates→B' lath-shaped precipitates and β rod-shaped precipitates [6]. Al-Mg-Si alloys DSC exothermal precipitations are studied and identified by TEM [7] [8] [9] [10]. There are 7 DSC exothermal peaks that are identified in a Al-Mg-Si alloy with high excess silicon. The suggested precipitation sequence is SSSS→independent Si and Mg atoms and clusters (peak 1)→GP zones (peak 2)→silicon rich phase (peak 3a)→β' (peak 3b)→β (peak 4)→silicon precipitates (peak 5)→β (peak 6) [11]. The DSC work on 6000-series alloy showed that the independent peak of clustering of Mg and Si atoms in the early stage of ageing was found at 30˚C ~ 110˚C. The GP zones of Mg and Si clustering precipitate in the range of 130˚C to 150˚C. The formation of β' produces a strong exothermic peak at ~250˚C. β and/or B' precipitates produce a peak at ~290˚C. The peak corresponding to Si precipitates was found at ~330˚C [11] [12]. The β Mg_2Si precipitation temperature with different interpretation had a peak temperature from 380˚C to 450˚C [9] [10]. The suggestion of exothermic peaks in the temperature range of 30˚C to 110˚C was attributed to clustering of Mg atoms and co-clustering of both Mg and Si atoms. No significant Si clusters and Si precipitates were observed. Si precipitates only in over-aged casting alloys of A356 and A357 [4].

Metastable clusters, β'', β and β phases are observed by DSC curves in which β'' precipitation plays the major role in improving hardness, but not β' precipitates. Increased Si content in the alloy had no obvious effect on the precipitation of β'' and B', but it did affect the formation of Si precipitates [12]. Lorella [13] suggest that room temperature pre-ageing 0 ~ 96 hours after quench will impact subsequent precipitation and reduce the hardness and strength 20% on a A356 alloy. The natural ageing process will cause a suppression in the formation of β'' phase during artificial ageing. This is due to the development of Mg and Si clusters that are stable at temperatures up to 180˚C. Clusters of Mg and Si transform into β'' phase at about 100˚C during artificial ageing.

Natural ageing suppresses the precipitation kinetics of the GP zones seen in artificial ageing, but pre-ageing at 70˚C increases the number density of the GP zones in the artificially aged alloy. This suggests that the GP zones formed in 70˚C during the preageing process conditions grow in the subsequent artificial ageing process, but the co-clusters formed by natural ageing are completely reverted [3]. The increase of natural ageing time at room temperature leads to a decrease in solute atoms and vacancies concentration in a solid solution. This results in a decrease in precipitation during subsequent heating processes. However, the pre-ageing will not impact the behavior of subsequent β'' phase precipitation. The pre-ageing at 120˚C could suppress the clustering process which is based on the suggestion that nuclei of β'' are formed during the pre-ageing process [10] [11] [12]. Edwards [5] [6] observed that the Mg and Si independent clusters are generated under natural ageing, the Mg and Si co-clusters are formed with longer natural time ageing. Under 70˚C isothermal pre-ageing, the Mg and Si clusters separate and disappear with time. They are then being replaced by co-clusters of Mg and Si atoms. Mg-Mg and Si-Si clusters are formed during or immediately after quenching. The Mg clusters tend to dissolve during room temperature ageing (1 week). Whereas, Si clusters still remain. A pre-ageing treatment at 363 K leads to a Mg-Si short-range correlation interpreted as the formation of Mg-Si mixed clusters. Therefore, Mg-Si co-clusters may act as preferential nucleation sites that lead to a higher density of hardening particles in the aged state and improve the paint-bake hardening response of the 6016 alloy [2].

Most of the previous studies focused on different composition and different pre-aging temperature impact on the precipitation process and precipitation phase identification. However, it had not yet been investigated whether or not integrating the quenching and pre-aging parameters influence on precipitation behaviors and mechanical properties of different Mg content alloys. Therefore, this paper will study the effects of quenching temperature and time, pre-ageing temperature and time effects on precipitation behaviors and the mechanical properties of Al-11Si, 6061, A356 and A357 alloys.

2. Experimental Procedure

Al-11Si, 6061 (Al-0.6Si-1Mg), A356 (Al-7.05Si-0.26Mg) and A357 (Al-6.95Si-0.63Mg) alloys were used in this study. The Al-11Si and 6061 alloys were bought from the commercial market. A356 and A357 alloys were cast in a steel mold with a 180 × 130 × 40 mm ingot size. The steel mold was baked to 400˚C before casting. The aluminum alloys were heated to 650˚C with the following nitrogen degas and de-dross treatment.

Test samples were treated at 540˚C for 6 hours solid solution, and then quenched in liquid nitrogen, 25 ˚C and 65˚C water, and 90˚C in a 5% NaOH solution, respectively. For 25˚C and 90 ˚C quenching, natural ageing samples were followed with 0, 48 hours or 15 days of 25 ˚C room temperature natural ageing treatment, respectively. On the other hand, in order to further investigate the effect of the 90˚C quenching process, A356 and A357 samples were quenched at 90˚C and immersed for 0, 1, 2 and 24 hours in water. The artificial heat treatment conditions used were 165˚C and 8 hours for A356 and 165˚C and 6 hours for A357, respectively.

DCS test samples 4 mm in diameter and 1 mm in thickness with weights around 20 mg were cut using a Fanuc wire cut machine. A SEIKO-DSC22C-SSC5100 DSC tester was utilized for calomeric testing. The temperature ramp rate was 10˚C/min, test sample heating range was from 40˚C to 572˚C. A 10 Ton MTS-810 test system was used and a ASTM B557-84 test standard was followed for tensile and elongation property measurement. The strain rate is 0.2 mm/min in the beginning. The strain rate is switched to 2 mm/min when strain reaches 1%.

3. Results and Discussions

3.1. Precipitation Behaviors of Alloys

Table 1 shows the Sparc's analysis result of Al-11Si, 6061, A356 and A357 alloy compositions. These 4 selected alloys were generated for DSC analysis. On the A356 and A357 alloy samples, tensile property tests were also conducted. Mg and Si solid solution weight percent are varied with solid solution temperatures. Based on phase diagrams, there is 0.61 wt% Mg and 0.85 wt% Si at solid solution at 540˚C. There is 0.26 wt% Mg and 0.85 wt% Si at solid solution for A356, 0.61 wt% Mg, 0.85 wt% Si for A357 and 0.61 wt% Mg and 0.85 wt% Si for 6061. Hence, there is 1.07 at % Mg_2Si that could be at solid solution at 540˚C for A356 alloys. There is 2.59 at % Mg_2Si that could be at solid solution at 540˚C for A357 and 6061 alloys. However for the necessary Si content necessary to form Mg_2Si stoichiometrically, there is an additional 0.7 wt% Si solid solution in A356 alloy, an additional 0.5 wt% Si solid solution in A357 alloy and an additional 0.02 wt% Si solid solution in 6061 alloy, respectively.

Figure 2 shows the DSC analysis results of Al-11Si, 6061, A357 and A356 alloys quenched to 25˚C in water without the natural ageing treatment. Based on the Al-Si alloy phase diagram, there is Si precipitation in Al-Si Alloy. From the Al-11Si DSC curve, there is an exothermal peak at 338.5˚C which peak is believed to be Si precipitation. There are 4 exothermal peaks at 81.8˚C, 251.9˚C, 301.9˚C and 498.3˚C for 6061 alloy. A357 has four exothermal peaks similar as well to the 6061 alloy, but in addition, there is an exothermal peak at 337.6˚C. Also, the 498.3˚C exothermal peak disappears when compared to the 6061 alloy. The additional exothermal peak (337.6˚C) after β precipitation is believed to be Si precipitation after comparison to the Al-11Si DSC curve which has a similar exothermic peak at 338.5˚C. Based on previous DSC studies [9] [10] [11] [12], the 81.8˚C is suggested to be Mg-Mg, Si-Si and Mg-Si clusters precipitation, the

Table 1. Composition of Al-11Si、6061、A356 and A357 alloys (in weight %).

Alloy	Si	Mg	Fe	Ti	Be	Cu	Zn	Mn	Sr	Sb	Al
Al-11Si	11.42	---	0.70	0.01	---	---	---	---	---	---	Rem
6061	0.60	1,00	---	---	---	---	---	0.28	---	---	Rem
A356	7.05	0.26	0.13	0.13	---	<0.01	0.01	<0.001	---	0.17	Rem
A357	6.95	0.63	0.10	0.13	0.04	<0.20	<0.10	<0.10	0.03	---	Rem

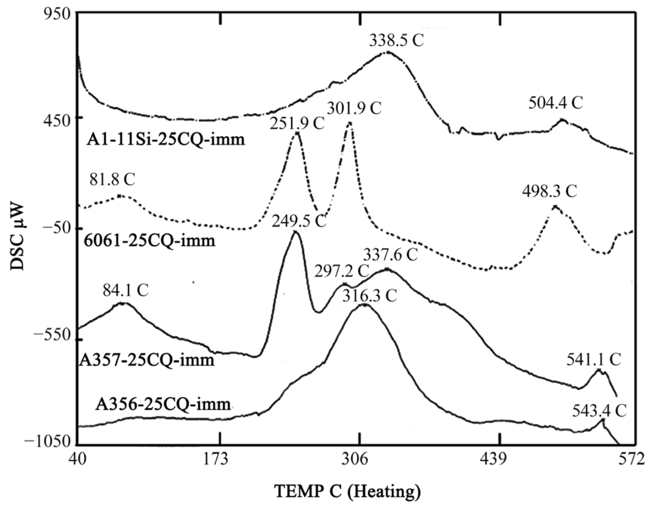

Figure 2. DSC analysis of Al-11Si, 6061, A357 and A356 alloys quenched in 25˚C water.

peak at 251.9˚C is β' precipitation, 301.9˚C is β and 498.3˚C is β precipitation. A357 DSC curve could be treated as the superposition of 6061 and Al-11Si DSC curves. The 541.1˚C exothermal peak could be caused by the superposition of β precipitation and Mg_2Si dissolution. For the A356 alloy, there is no obvious exothermal peak at 81.8˚C and not any clear exothermal peaks at 251.9˚C, 301.9˚C and 337.6˚C. Without clear Mg-Mg, Si-Si and Mg-Si clusters, β' and β precipitation exothermal peaks are believed due to the fact that A356 has less Mg supersaturation than A357. It was possible to identify the full A356 DSC precipitation process by quenching the alloy in liquid nitrogen and starting a DSC thermalgram measurement from −50˚C, as shown in **Figure 3**. Compared to the DSC curve of A357, there are still no clear Mg-Mg, Si-Si and Mg-Si cluster precipitation peaks in the A356 alloy. However, there is a small precipitation starting from −30˚C. The composition difference between A356 and A357 is that A356 has less Mg supersaturation. It is believed that low Mg supersaturation which causes the A356 DSC curve result shows almost no Mg-Mg cluster exothermic peak after quench.

Figure 4 shows the DSC analysis of A357 quenched to 25˚C, then treated with 0 and 48 hours and 15 days room temperature pre-ageing. The thermal diagrams are similar to the previous DSC studies [11] [12]. There are 6 peaks identified. Cluster (peak 1), GP zone (peak 2), β' (peak 3a and 3b), β (peak 4) and Si precipitation exothermic peak (peak 5) for the alloy without natural ageing. The differences are that the Mg-Mg cluster endothermic peak and β exothermic peak (peak 6) cannot be identified. The alloy begins to melting at temperature of 535.2˚C as we can be found in **Figure 4**. The cluster exothermal and endothermal volumes are reduced and also peak temperatures are increased for the alloy after 48 hours and 15 days natural ageing. However, the Si exothermal peak temperature was decreased along with natural ageing time increasing, then when superimposed with β exothermal peak to be one exothermal peak for the sample

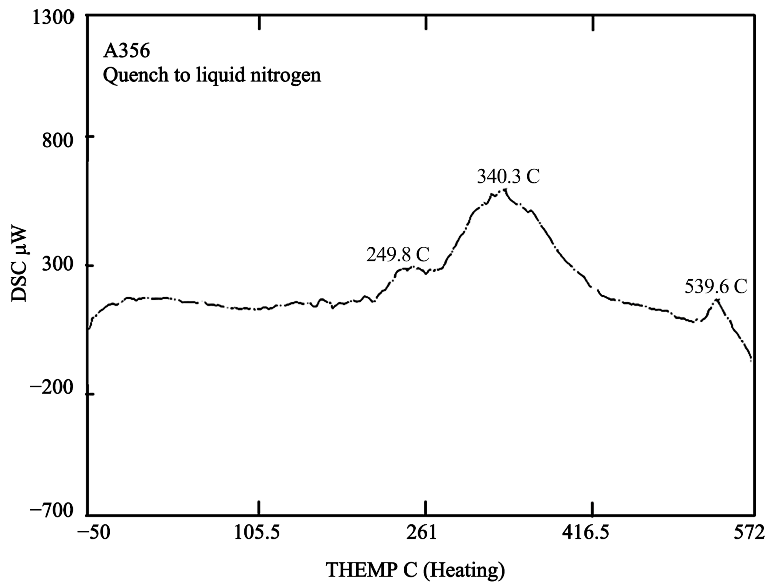

Figure 3. DSC analysis of A356 quenched in liquid nitrogen.

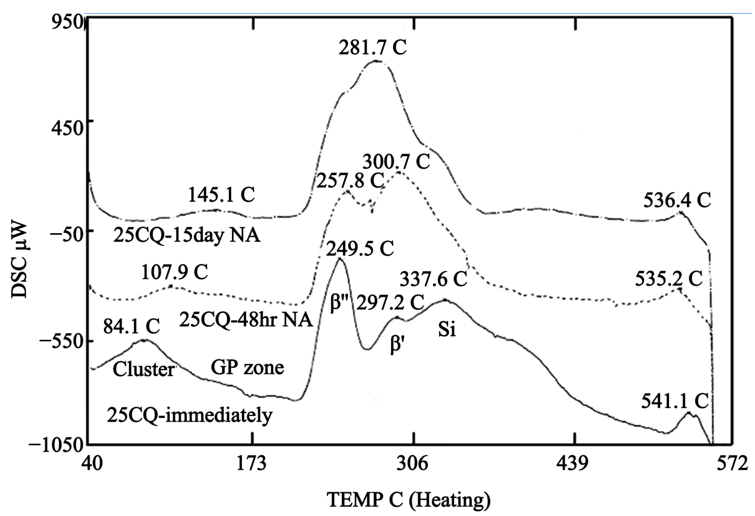

Figure 4. DSC analysis of A357 quenched to 25˚C, then treated with 0 and 48 hours and 15 day room temperature pre-ageing.

with 48 hours natural ageing. In natural ageing 15 day sample, the cluster exothermal peak temperature is increased and precipitation volume is reduced. From DSC thermalgram of alloy without natural ageing, the precipitation sequence is Mg-Mg, Si-Si and Mg-Si cluster precipitation, Mg-Mg cluster dissolution, GP zone precipitation and then β' precipitation [2]. The Mg-Mg clusters dissolved at higher temperature, which could provide higher Mg solid solution supersaturation. Hence, the β' exothermal precipitation peak temperature is lower and exothermal peak area is higher than the 48 hour and 15 day natural aged samples [9]. Along with the natural ageing time increase, the Mg-Si cluster exothermal peak temperature is increased, but its area is reduced. Simultaneously, at the Mg-Mg endothermal peak is reduced. The Mg-Si cluster exothermal peak temperature is increasing along with natural ageing time increase.

The Mg-Si cluster is stable which is not dissolved along with DSC temperature increase. For 48 hours and 15 days natural aged samples, there are more Mg-Si stable clusters precipitated. This reduces Mg-Si cluster precipitation peak size and reduces the Mg-Mg cluster endothermal peak size as well. Due to Mg and Si supersaturation being reduced after natural ageing, the β' exothermal peak size is reduced and its precipitation peak temperature is increased. Increasing the natural ageing time will cause Si exothermal peak temperature reduction. β and Si exothermal peaks are superimposed to become one exothermal peak which shows up on the 48 hour natural aged DSC thermalgram. Along with natural ageing time increases, the Si exothermal peak temperature is reduced from 337.7˚C to 281.7˚C, β', β and Si are superimposed as one large exothermal peak. These A357 DSC analysis curves agree with the previous study of Zhen [11]. Precipitation particles of samples without natural ageing are finer and denser than that of samples with natural ageing. Natural ageing will cause Mg-Si cluster precipitation but without dissolution which reduces Mg and Si supersaturation which then delays β' precipitation [10].

Figure 5 shows the DSC analysis of A357 quenched to 90˚C for 0 and 48 hours and 15 days room temperature pre-ageing. Part of the Mg-Si cluster and β' precipitation peaks overlap each other without natural ageing of the alloy. When conducting 48 hour and 15 day natural ageing alloy samples, the Mg-Si cluster exothermal peak temperature increases along with natural ageing time increase and its β' phase exothermal peak temperature is increased as well. However, the β and Si precipitation exothermal peak temperature was reduced along with naturals ageing time increase which is caused by Si exothermal peak temperature reduction. The longer the natural ageing time, the more the Si exothermic temperature drops. A 90˚C quench promotes Mg-Si cluster precipitation. Natural ageing increases the Mg-Si cluster exothermal peak. A longer natural ageing time results in a higher Mg-Si and β' precipitation temperature, as shown in **Figure 4** and **Figure 5**, respectively.

Figure 6 shows the DSC analysis of A357 quenched to 90˚C for 0, 1, 2 and 24 hours, respectively. The Mg-Si cluster and β' precipitation volume was reduced along with quench time increases. This suggests that the 90˚C quench could promote Mg-Si cluster and β' precipitation. The β' exothermal temperature increases with 90˚C preageing time increases due to Mg and Si solid solution supersaturation being reduced following the 90˚C pre-ageing increase. The β precipitation exothermal peak increases along with 90˚C quench time increases. The Si precipitation exothermal peak is reduced from 340.1˚C to 329.2˚C along with 90˚C quench time increases from 0 to 24 hours.

Figure 7 shows the DSC analysis of A357 quenched to 90˚C for 24 hours, then treated with 0 and 48 hours and 15 days natural ageing. The β', β and Si exothermal peak temperatures are similar even after different natural ageing. It is believed that 90˚C pre-ageing of 24hours could cause Mg-Si cluster and β' precipitation which then reduces Mg/Si and vacancy supersaturation that eliminates the natural ageing impact.

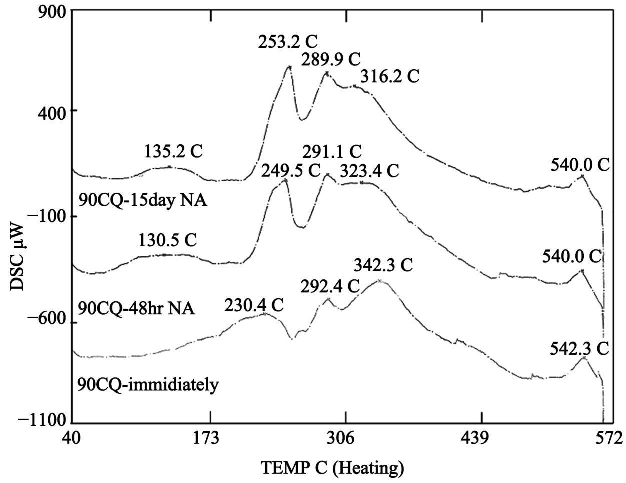

Figure 5. DSC analysis of A357 quenched to 90˚C for 0 and 48 hours and 15 day room temperature pre-ageing.

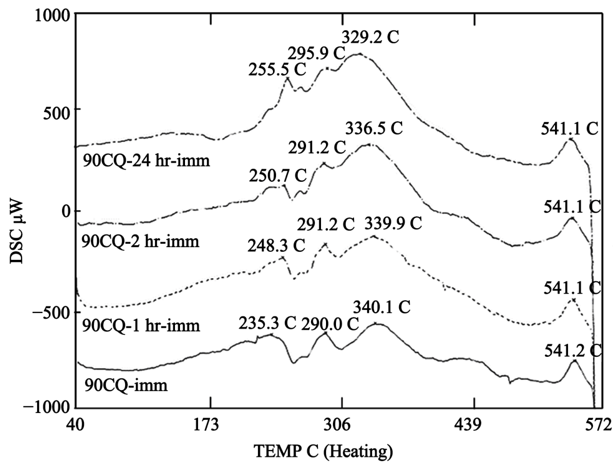

Figure 6. DSC analysis of A357 quenched to 90˚C for 0, 1, 2 and 24 hours, respectively.

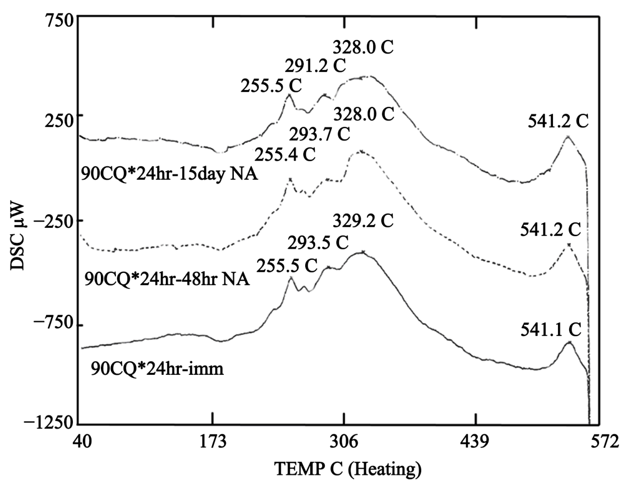

Figure 7. DSC analysis of A357 quenched to 90˚C for 24 hours, then treated with 0 and 48 hours and 15 day room temperature pre-ageing.

Compared with A357 alloy quenched to 25˚C and 90˚C, studies of Figure 4 and Figure 5, for A356 alloy in which Mg-Mg, Si-Si, Mg-Si cluster, *β*', *β* and Si exothermal and precipitation peaks are superimposed together, as shown in Figure 8 and Figure 9. There are no obvious cluster exothermal peaks for quenching to 25˚C and 90˚C samples and in additon for 48 hour or 15 day natural aged samples. The only composition difference between A356 and A357 alloys is Mg content. A356 alloy has lower Mg content (0.26 wt%) compare to A357 (0.63 wt%). The higher Mg content will cause more Mg-Mg cluster precipitation. There is less Mg in A356 in which there are no obvious Mg-Mg and Mg-Si cluster precipitations. Hence, A356 has less natural ageing effect on the mechanical properties compared to A357 which suggest less Mg-Si cluster precipitation due to less Mg supersaturation. Separate *β*' and *β*/Si peaks are observed

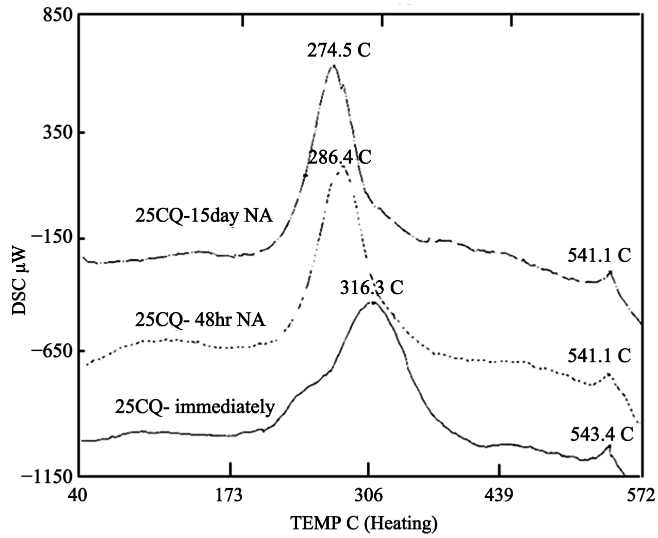

Figure 8. DSC analysis of A356 quenched to 25˚C, then treated with 0 and 48 hours and 15 day room temperature pre-ageing.

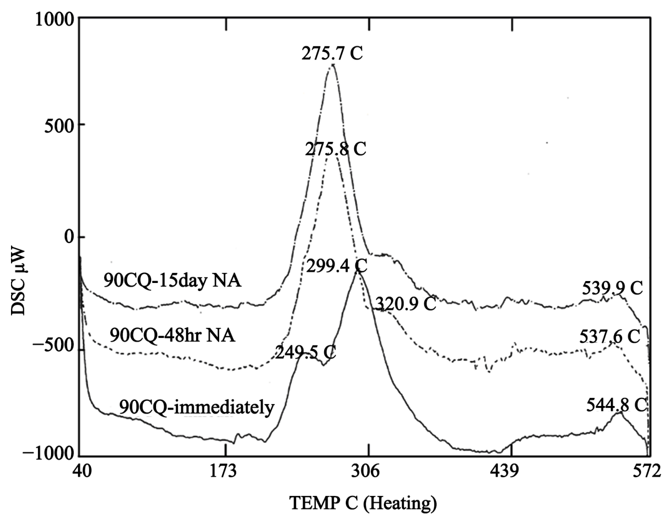

Figure 9. DSC analysis of A356 quenched to 90˚C, then treated with 0 and 48 hours and 15 day room temperature pre-ageing.

for A356 alloy quenched to 90˚C without natural ageing. The superposition precipitation peak temperature is decreased with natural ageing time increase. Based on the previous A357 study of Figure 4 and Figure 5, the peak temperature decrease is due to Si exothermal peak temperature decrease with natural ageing. In the A356 alloy study of Figure 8 and Figure 9, the Si exothermal peak temperature reduction is quicker than in A357. Figure 10 shows the A356 alloy quench at 90˚C for 0, 1, 2 and 24 hours, respectively, the β' precipitation volume is reduced along with quenching time increases as well.

3.2. Mechanical Properties of Alloys

Figure 11 shows the tensile properties of A356 and A357 alloys after 25, 65 or

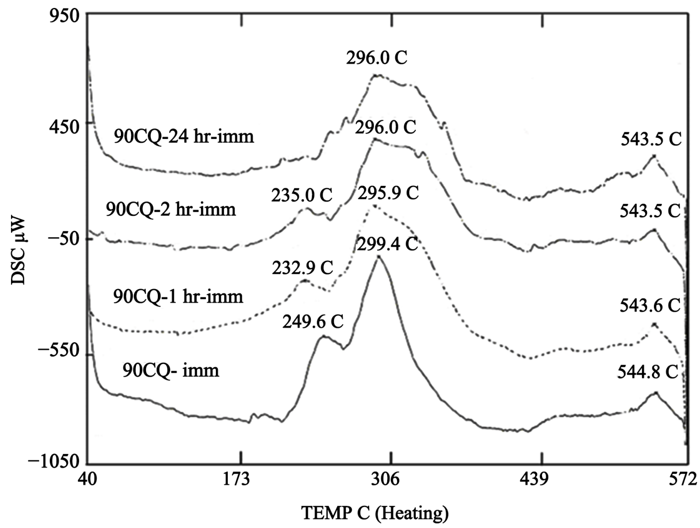

Figure 10. DSC analysis of A356 quenched to 90˚C for 0, 1, 2 and 24 hours, respectively.

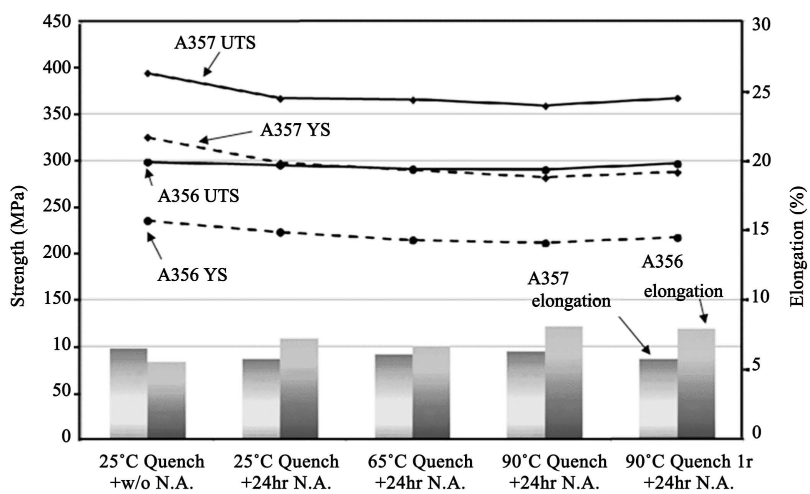

Figure 11. Tensile properties of A356 and A357 alloys, after 25˚C quench (then with 0 and 24 hours natural ageing), after 65˚C and 90˚C quench (then with 24 hours natural ageing), after 90˚C quench for 1 hour (then with 24 hours natural ageing).

90˚C quench temperatures, and then with 0 or 24 hours natural ageing. The highest UTS and YS values (condition: 25˚C Quench + w/o N.A.) were obtained when both A356 and A357 alloys are quenched to 25˚C, but without the natural ageing treatment. The strength is reduced for both A356 and A357 alloys with natural ageing. Compared with condition: 25˚C Quench + w/o N.A., after 24 hours natural ageing (condition: 25˚C Quench + 24hr N.A.), the tensile strength of UTS or YS is reduced 1.4% and 5.1% for A356. There is 6.9% and 8.6% reduction for A357 alloy. A356 is less impacted by natural ageing than A357. This suggest that A356 has less Mg-Mg and Mg-Si cluster precipitation during natural ageing, as demonstrated in **Figure 4** and **Figure 9**.

With both A356 or A357 alloys, the increase of quench temperature from 25˚C to 90˚C will result in a decrease in UTS, YS and an increase in elongation. This corresponds to a decrease in the Mg and Si supersaturation, usually associated with an increase in quench temperature.

The 90˚C pre-ageing can promote β' precipitation if its immersion time is enough. **Figure 6** (A357 alloy) and 10 (A356 alloy) demonstrate the longer the 90˚C pre-ageing time results, This results in more β' precipitation which shows the β' precipitation reduction on the DSC thermograms. Hence, the increase of 90˚C pre-ageing time in A356 and A357 alloys, from 0 (condition: 90˚C Quench + 24hr N.A.) to 1 (condition: 90˚C Quench 1hr + 24hr N.A.) hour, results in an increase in UTS and YS and a decrease in elongation, as shown in **Figure 11**. The increase in UTS and YS and a decrease in elongation is explained by the higher β' precipitation of A356 and A357 alloys using the longer 90˚C pre-ageing time.

4. Conclusions

Based on DSC analysis, the precipitation processes are as suggested below.

a) For room temperature quench, but without natural ageing, the precipitation process is: SSSS→Mg-Mg/Si-Si cluster→Mg-Mg cluster dissolution→Mg-Si cluster →β'→β→Si→β.

b) For room temperature quench, but with long natural ageing, the precipitation process is: SSSS→ Mg-Si cluster→β'→β→Si→β.

c) For 90˚C quench and pre-ageing precipitation, the process is: SSSS→ Mg-Si cluster and β'→β→Si→β.

Natural ageing will induce Mg-Si cluster precipitation to consume supersaturation, which reduces artificial treatment mechanical strength. A 90˚C pre-ageing process will promote Mg-Si cluster precipitation to critical size and β' precipitation to mitigate the natural ageing impact on artificial treatment. There is a minor natural ageing impact on A356 alloy cluster formation compared to A357 alloy, due to less Mg-Mg and Mg-Si cluster formation.

The Mg-Mg cluster will be dissolved before β' precipitates in the alloys without natural ageing. The natural ageing will delay Mg-Si cluster, β' and β precipitation but promote Si precipitation. The 90˚C pre-ageing temperature will promote Mg-Si clusters and β' precipitation directly. When increasing the 90˚C pre-ageing time, there will be more Mg-Si cluster and β' precipitation which will cause the alloys to have higher tensile strength.

References

[1] Banhart, J., Sin, C., Chang, T. and Liang, Z. (2010) Natural Ageing in Al-Mg-Si Alloys—A Process of Unexpected Complexity. *Advanced Engineering Materials*, **12**, 559-571. https://doi.org/10.1002/adem.201000041

[2] Geuser, F.D., Lfebvre, W. and Balvette, D. (2006) 3D Atom Probe Study of Solute Atoms Clustering during Natural Ageing and Pre-Ageing of an Al-Mg-Si Alloy. *Philosophical Magazine Letters*, **86**, 227-234. https://doi.org/10.1080/09500830600643270

[3] Murayama, M. and Hono, K. (1999) Precipitate Clusters and Precipitation Processes in Al-Mg-Si Alloys. *Acta Materialia*, **47**, 1537-1548. https://doi.org/10.1016/S1359-6454(99)00033-6

[4] Sha, G., Möller, H. and Stumpf, W.E. (2012) Solute Nanostructures and Their Strengthening Effects in Al-7Si-0.6Mg Alloy F357. *Acta Materialia*, **60**, 692-701. https://doi.org/10.1016/j.actamat.2011.10.029

[5] Edwards, G.A., Stiller, K. and Dunlop, G.L. (1994) APFIM Investigation of Fine-Scale Precipitation in Aluminum Alloy 6061. *Applied Surface Science*, **76/77**, 219-225. https://doi.org/10.1016/0169-4332(94)90346-8

[6] Edwards, G.A., Stiller, K. and Dunlop, G.L. (1998) The Precipitation Sequence in Al-Mg-Si Alloys. *Acta Materialia*, **46**, 3893-3904. https://doi.org/10.1016/S1359-6454(98)00059-7

[7] Takeda, M., Ohkubo, F. and Shirai, T. (1998) Stability of Metastable Phases and Microstructures in the Ageing Process of Al-Mg-Si Ternary Alloys. *Journal of Materials Science*, **33**, 2385-2390. https://doi.org/10.1023/A:1004355824857

[8] Takeda, M., Kurumizawa, T., Sumen, S., Fukui, K. and Endo, T. (2002) Atomic Composition of the Metastable β" Phase Precipitate in an Al-Mg-Si Alloy. *Zeitschrift für Metallkunde*, **93**, 523-527. https://doi.org/10.3139/146.020523

[9] Gupta, A.K. and Lloyd, D.J. (1999) Study of Precipitation Kinetics in a Super Purity Al-0.8 Pct Mg-0.9 Pct Si Alloy Using Differential Scanning Calorimetry. *Metallurgical and Materials Transactions A*, **30A**, 879-884. https://doi.org/10.1007/s11661-999-1021-9

[10] Esmaleli, S., Wang, X., Lloyd, D.J. and Poole, W.J. (2003) On the Precipitation-Hardening Behavior of the Al-Mg-Si_Cu Alloy AA6111. *Metallurgical and Materials Transactions A*, **34A**, 751-763.

[11] Zhen, L. and Kang, S.B. (1998) DSC Analysis of Precipitation Behavior of Two Al-Mg-Si Alloys Naturally Aged for Different Times. *Materials Letters*, **37**, 349-353. https://doi.org/10.1016/S0167-577X(98)00118-9

[12] Zhen, L., Kang, S.B. and Kim, H.W. (1997) Effect of Natural Ageing and Preageing on Subsequent Precipitation Process of an Al-Mg-Si Alloy with High Excess Silicon. *Materials Science and Technology*, **13**, 905-910. https://doi.org/10.1179/mst.1997.13.11.905

[13] Ceschini, L., Morri, A. and Morri, A. (2013) Effects of the Delay Between Quenching and Aging on Hardness and Tensile Properties of A356 Aluminum Alloy. *Journal of Materials Engineering and Performance*, **22**, 200-205. https://doi.org/10.1007/s11665-012-0208-1